Biochimica et Biophysica Acta, 1057 (1991) 299–312

ADONIS 000527289100102C

BBABIO 43370

Temperature dependence of the initial electron-transfer kinetics in photosynthetic reaction centers of *Chloroflexus aurantiacus*

M. Becker [1], V. Nagarajan [1], D. Middendorf [1,*], W.W. Parson [1], J.E. Martin [2] and R.E. Blankenship [2]

[1] *Department of Biochemistry, University of Washington, Seattle, WA and* [2] *Department of Chemistry, Arizona State University, Tempe, AZ (U.S.A.)*

(Received 1 October 1990)
(Revised manuscript received 28 December 1990)

Key words: Electron transfer; Reaction center; Photosynthetic bacterium; (*Chl. aurantiacus*)

Absorbance changes in the near infrared were measured in photosynthetic reaction centers of the thermophilic, gliding, green bacterium *Chloroflexus aurantiacus* over the temperature range from 80 to 320 K, using 605-nm excitation pulses with an autocorrelation width of about 0.8 ps. Spectra collected during the first 1.5 ps after excitation show stimulated emission from the excited singlet state P*, absorbance increases at 762 and 802 nm, and absorbance decreases in the 865-nm band and at 783 and 815 nm. The absorbance changes associated with the formation of P* suggest that the electronic transitions in the ground-state spectrum are strongly mixed. Spectra collected up to 90 ps after the excitation pulse show the decay of the stimulated emission, and bleaching at 750 nm and 815 nm, reflecting the transfer of an electron from the bacteriochlorophyll dimer (P) to the initial electron acceptor(s). The electron-transfer reaction is slower in *C. aurantiacus* than in reaction centers of purple bacterial species; P* decays with a time-constant of 7.1 ± 0.5 ps at 296 K and 9.0 ± 0.1 ps at 320 K. At lower temperatures, the kinetics are non-exponential. The decay of the stimulated emission at 80 K can be fit either with a biexponential function with time constants of 3.0 ± 0.1 and 32 ± 12 ps, or with a stretched exponential function [$\exp - (t/\tau_0)^{\alpha}$] with $\tau_0 = 4.1 \pm 1.2$ ps and $\alpha = 0.45 \pm 0.06$. Several models that might account for the nonexponential decay kinetics of P* are discussed. A model based on rapid interconversion among conformational states in P* provides a simple interpretation of the temperature dependence of the kinetics.

Introduction

The thermophilic, gliding, green bacterium *Chloroflexus aurantiacus* may be a representative one of the earliest branches in the evolution of photosynthetic organisms [1]. Its antenna system and membrane structure are similar to those of the green sulfur bacteria, but its photosynthetic reaction center (RC) resembles reaction centers of the purple bacteria.

Photosynthetic RCs of the purple bacteria generally contain three polypeptides, designated L, M and H, with molecular weights of about 31000, 34000, and 28000, respectively [2]. The protein binds four bacteriochlorophylls (BChl), two bacteriopheophytins (BPh), two quinones (Q), and a non-heme iron. Crystal structures have been solved for RCs of *Rhodopseudomonas viridis* and *Rhodobacter sphaeroides* [3–6]. Both strutures contain a closely interacting pair of BChls (P), from which extend two branches of pigments, the 'L' or 'A' branch and the 'M' or 'B' branch. Each branch of pigments has a BChl nearest to P, followed by a BPh, and then a quinone. Studies on *Rb. sphaeroides*, *Rp. viridis* and *Rb. capsulatus* have shown that, after absorbing a photon, P transfers an electron to a BPh (H_L) in about 3.5 ps [7–16]. It is not yet clear whether the 'accessory' BChl (B_L) between P and H_L serves as an intermediate electron carrier in this reaction [7–15,17–20]. An electron moves from the reduced BPh (H_L^-) to one of the quinones (Q_A) in about 230 ps [21], forming $P^+Q_A^-$ with a quantum yield of essentially 1.0 [22]. The rates of the initial electron-transfer reactions increase as the temperature is lowered [7,16,21,23]. Although the arrangements

Abbreviations: BChl, bacteriochlorophyll; BPh, bacteriopheophytin; LDAO, lauryldimethylamine oxide; PVA, polyvinylalcohol; RC, reaction center.

* Present address: The Evergreen State College, Olympia, WA, U.S.A.

Correspondence: W.W. Parson, Department of Biochemistry, SJ-70, University of Washington, Seattle, WA 98195, U.S.A.

of the pigments and the amino acids on the L and M branches are similar, only H_L ordinarily undergoes photoreduction [24,25].

Chloroflexus aurantiacus RCs share many of the properties of RCs of purple bacteria but have some significant differences. They contain two polypeptides with molecular weights of about 35 000, which are homologous to the L and M subunits [26–28]. An H-subunit apparently is lacking. Spectral analysis, pigment extraction, and comparisons of the amino acid sequences have shown that RCs of *C. aurantiacus* contain 3 BChls and 3 BPhs instead of 4 BChls and 2 BPhs [27–30]. Whereas RCs of most species of purple bacteria contain an iron atom, and either two ubiquinones or one ubiquinone and one menaquinone, RCs of *C. aurantiacus* contain manganese and two menaquinones [31–33]. Also, *C. aurantiacus* RCs are more stable than those of *Rb. sphaeroides* at elevated temperatures [34].

As in the purple bacteria, the primary electron donor in *C. aurantiacus* is a BChl dimer [35]. Spectroscopic measurements and comparisons of the amino acid sequences suggest that the pigments in *C. aurantiacus* are arranged similarly to the pigments in *Rp. viridis* and *Rb. sphaeroides*, except that the accessory BChl on the M-side is replaced by BPh [27,28,36–38]. The absorbance changes associated with the formation of $P^+Q_A^-$ in *C. aurantiacus* are slightly different from those seen in *Rb. sphaeroides* [29,36–43], and the electron-transfer reactions are somewhat slower. Kirmaier et al. [41] found that electron transfer from BPh^- to Q_A proceeds with a time constant of about 320 ps in *C. aurantiacus*, which is about 50% slower than in *Rb. sphaeroides*, and they noted that the initial reduction of BPh also appeared to be slower. Preliminary studies in this laboratory showed that BPh is reduced with a time constant of about 8 ps at room temperature [44]. On the basis of data obtained with 33-ps pulses, Shuvalov et al. [43] suggested that BChl is reduced first, with a time constant 10 ps, and that an electron then is transferred to BPh in 3 ps.

The present investigation examines the primary electron transfer kinetics in *C. aurantiacus* RCs over a wide temperature range with improved time resolution. A preliminary account of some of this work has been presented previously [45].

Materials and Methods

Chloroflexus aurantiacus strain J10-fl was obtained from the American Type Culture Collection and grown in a 12 liter glass-walled fermenter under 1000–1200 W incandescent illumination. Medium DG of Pierson and Castenholz [46] was modified by replacing the glycylglycine with 1.01 g/l of trizma base as buffer. Cultures were routinely checked for purity by light microscopy.

Reaction centers were prepared essentially as described by Blankenship et al. [47], with the following modifications: The supernatant liquid obtained by treating membranes with 1.5% lauryldimethylamine oxide (LDAO) was dialyzed against 50 mM Tris (pH 9.0)/0.1% LDAO and applied to a Sepragen Superflo-500 radial flow column packed with Pharmacia DEAE-Sephacel. The column was washed extensively with 50 mM Tris (pH 9.0)/0.2% LDAO until the green color due to solubilized antenna pigment BChl-c was removed. Reaction centers were eluted by increasing the NaCl concentration to 50 mM. The DEAE chromatography was repeated on a 2.5×18 cm column, and final purification was achieved by passing the RCs through an S-300 gel filtration column (2.5×30 cm) in 20 mM Tris (pH 8.0)/0.05% LDAO. The RCs were concentrated on an Amicon ultrafilter with a YM-30 membrane. This procedure yielded RCs with a 280 nm/812 nm absorbance ratio of 1.4 to 1.5.

For measurements at high temperatures, RCs were dialyzed into 0.6% Deriphat, 0.0125% LDAO, 20 mM Tris HCl (pH 8.0). These conditions were found to maximize the stability of *C. aurantiacus* RCs at high temperatures (Huxel, G. and Blankenship, R.E., unpublished observations). For most of the measurements at low temperatures, RCs were embedded in poly(vinyl alcohol) (PVA) films [48]. To examine the effect of pH, RCs were dialyzed against 0.05% LDAO and 40 mM pyrophosphate at the desired pH, concentrated by pressure dialysis, and mixed with glycerol (60% v/v). Because the volumes of the samples were too small for the final pH to be measured directly, we measured the pH of similar mixtures of glycerol and buffer lacking RCs.

For measurements at room temperature, samples were pumped continuously from a cooled sample reservoir through a cuvette with a 1 mm pathlength. For higher temperatures, the cuvette and reservoir were housed in a heated styrofoam chamber. For low temperatures, samples were cooled in the dark in a liquid-N_2 dewar. The temperature was measured with a thermocouple attached to the surface of the cuvette or film holder. Temperature fluctuations were about ± 1 K at room temperature and higher, and about ± 5 K at low temperatures. Sample absorbances at 296 K ranged from 0.7 to 1.4 at 813 nm. Degradation during the course of each experiment was negligible, as judged by ground-state absorption spectra. Ground-state spectra were measured with a Shimadzu UV-160 spectrophotometer equipped with a dewar.

Time-resolved absorbance measurements were made using 605-nm excitation flashes with an autocorrelation width of about 0.8 ps. The system was essentially as described [7,49], with the exception that the two probe beams were directed through separate monochromators onto linear arrays of 512 photodiodes (Hamamatsu 2301–512Q). The exit slits were removed from the

monochromators to allow dispersion of a spectrum covering approximately 300 nm onto each array. When necessary, neutral density filters were placed in the probe beams to prevent saturation of the diodes. The outputs from the diode arrays were amplified, digitized with a 12-bit analog-to-digital converter, and transferred to a computer.

To improve the signal-to-noise ratio in the spectra and to avoid saturation effects, the signals on each laser flash were accepted only if the maximum and minimum photovoltages from the diode arrays fell within defined bounds. Typically 50% to 90% of the laser flashes were accepted. Each of the spectra shown below represents an average of 500 accepted flashes. Dark currents from the diodes were subtracted before the calculation of absorbance changes. The diode arrays were calibrated with sharp-band interference filters, and also with a krypton lamp. The estimated error in wavelength determination is ± 1.5 nm. Chirping across the spectra is estimated to be about 1 ps.

The excitation flash typically bleached about 20% of the 865-nm band in the ground-state spectrum. Spectra were collected in 0.25-ps intervals at early times relative to the excitation pulse, and in steps as large as 2 ps at later times. The uncertainties for time constants reported in the text were calculated by averaging time constants from experiments on two to four different samples at each temperature.

Results

Spectra and kinetics at physiological temperatures

Figure 1a shows the ground-state absorption spectrum of *C. aurantiacus* RCs in solution at 320 K. Figs. 1b and 1c show picosecond difference spectra obtained with a similar sample at various times between -0.75 and 90 ps relative to an excitation flash. The spectra collected up to 1.5 ps after excitation (Fig. 1b) include a bleaching of the long-wavelength absorption band at 865 nm, stimulated emission from P* [7,44] in the region of 910 nm, and small absorbance decreases at 815 and 783 nm. Absorbance increases occur at 762 and 802 nm, and below 760 nm. Spectra collected at later times (Fig. 1c) show decay of the stimulated emission, growing absorbance decreases at 750 and 815 nm, and an absorbance increase at 795 nm. The absorbance changes in the region from 750 to 815 nm are associated with electron transfer from P* to the initial electron acceptors [7]. Absorbance changes measured at 296 K with RCs in solution or in PVA films were similar to those shown in Fig. 1, except that the bleaching of the 865-nm band was shifted by about 4 nm to longer wavelengths.

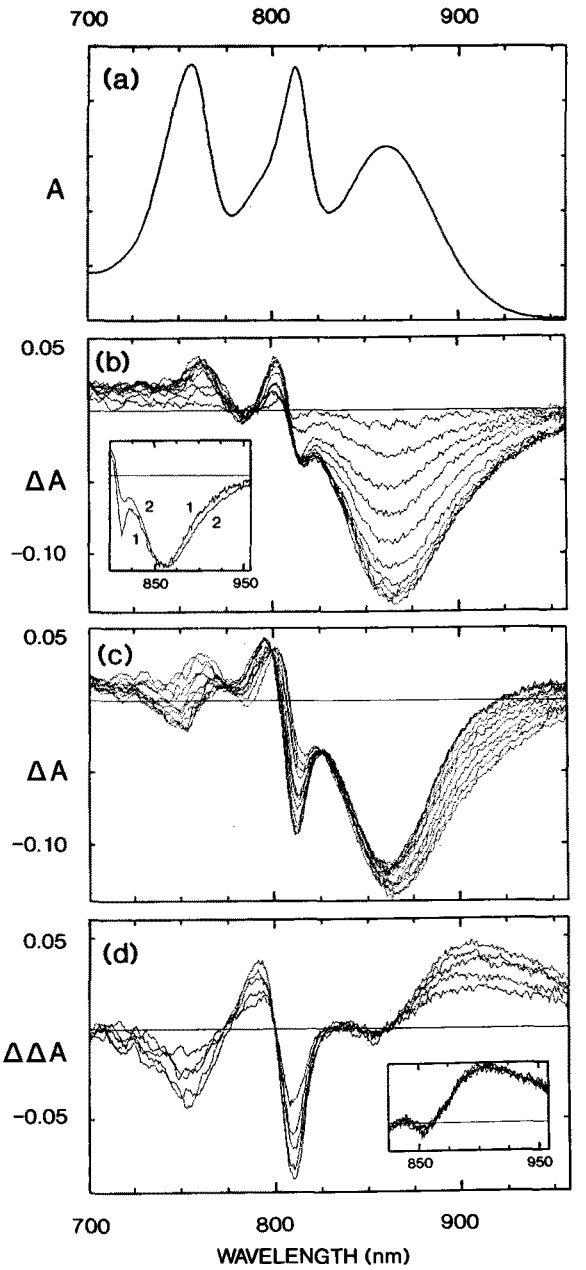

Fig. 1. Spectra of *C. aurantiacus* RCs in 0.6% Deriphat, 0.125% LDAO, 20 mM Tris HCl (pH 8.0) at 320 K. (a) Ground-state spectrum. (b) Difference spectra measured at various times between -0.75 ps and 1.5 ps relative to the excitation flash. Sample A at 813 nm = 0.97. Inset: Spectra at -0.25 ps (curve 1) and 1.5 ps (curve 2), normalized at 865 nm. (c) Difference spectra measured at selected times between 1.5 ps to 90 ps. (d) Stimulated-emission spectra obtained by subtracting spectra measured at 2, 3.25, 4.5, 6, and 9 ps from the average of the spectra measured between 70 and 90 ps. Inset: same spectra, normalized at 910 nm.

To characterize the kinetics, the data were fit to a multiexponential function of the form

$$S(t) = E(t-\delta) \otimes \left(\sum_i A_i e^{-t/\tau_i} + B \right) \quad (1)$$

where $S(t)$ is the calculated signal at time t, τ_i and A_i are the lifetime and amplitude of component i, $E(t)$ is

an excitation function, B is a constant, and $\otimes$ denotes a convolution [7]. $E(t)$ was generated separately for each data set by fitting a $\mathrm{sech}^2(t)$ function to the first derivative of the "instantaneous" bleaching near 855 nm. The phase shift δ is included to accommodate the small chirping of the probe pulses as they pass through dispersive materials prior to the sample.

Fig. 2a shows the decay kinetics of the stimulated-emission signal at 320 K. The decay of P* is described well by a single-exponential function. Measurements at other wavelengths between 875 and 950 nm showed similar kinetics. The time constant obtained by averaging fits at 10-nm intervals across the emission band in two experiments was 9.0 ± 0.1 ps.

A single exponential also was sufficient to describe the kinetics of stimulated emission at room temperature (296 K). Samples in Deriphat-LDAO solutions, in 0.05% LDAO alone, or in PVA films all gave similar results. Including measurements in all of these media and at wavelengths across the emission band, the average time constant at 296 K was 7.1 ± 0.5 ps.

With RCs in solution at either 296 or 320 K, the time constants were about 1 ps longer on the long-wavelength edge of the stimulated-emission band than on the short-wavelength edge. This suggests that the signals could contain unresolved kinetic components whose relative amplitudes depend on wavelength; however, fits to a biexponential function either gave two time constants that were essentially the same as the time constant obtained with a single exponential, or gave one similar time constant and a component that was nonsystematically much longer or much shorter. (Data obtained with PVA films at 297 K had a lower signal-to-noise ratio than the data obtained with solutions or with PVA films at low temperatures, but could be fit by either a single- or bi-exponential function with similar values of the reduced χ^2; the biexponential fits gave time constants of 4.1 ± 1.0 ps and 13 ± 1 ps.)

An apparent dependence of the kinetics on wavelength could result from a shift of the stimulated-emission spectrum to longer wavelengths with time. Such shifts are seen with monomeric BChl in solution [50], and might be expected to occur in RCs as a result of nuclear relaxations in the excited state. Spectra of the stimulated emission from RCs can be calculated for various times after the excitation pulse by subtracting the measured difference spectra from a spectrum measured at a much later time (Fig. 1d). The inset in Fig. 1d shows that, when the calculated emission spectra are normalized near 910 nm, the spectra at times later than 1.5 ps after the excitation pulse are indistinguishable within the experimental error. Any shifting of the stimulated-emission spectrum thus appears to be essentially complete within about 1.5 ps. To calculate stimulated-emission spectra from data collected during the excitation pulse, the early spectra must be normalized

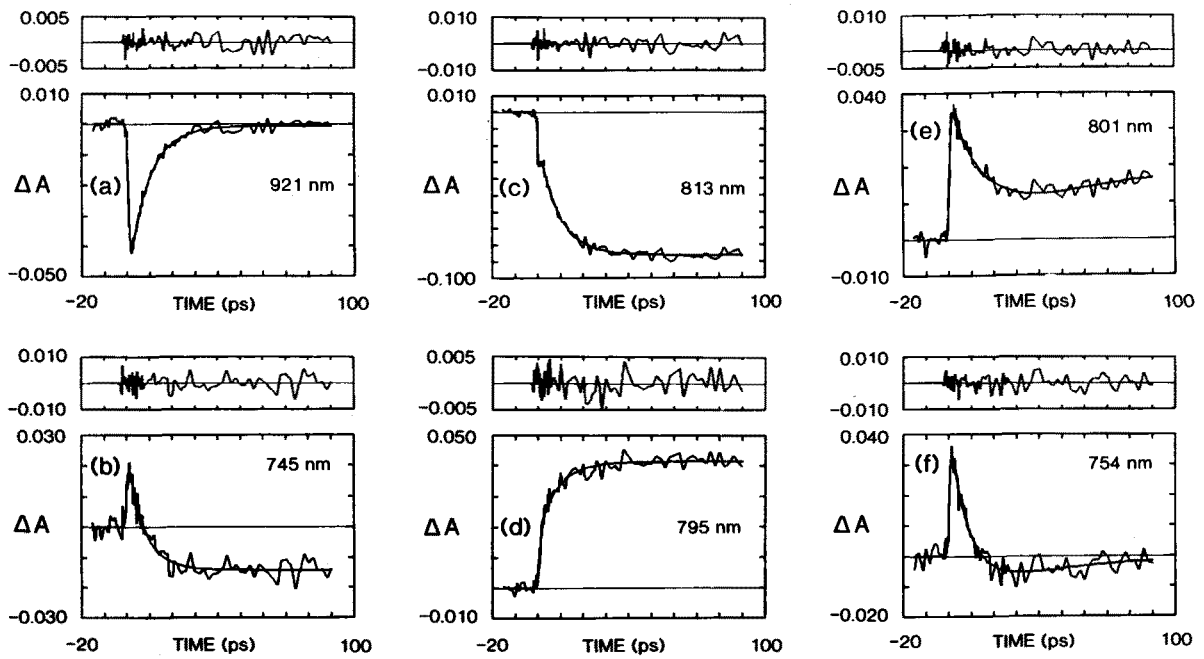

Fig. 2. Kinetics at 320 K. The trace shown in (a) represents an average over 10-nm slices of spectra like those shown in Fig. 1; those in (b) to (f) are averages over 5 nm. The smooth curves drawn through the data show fits to single- or double-exponential expressions with the following time constants (for the double-exponential fits, the numbers in parenthesis are the relative amplitudes of the components): (a) 921 nm, $\tau = 9.1$ ps. (b) 745 nm, $\tau = 7.4$ ps. (c) 813 nm, $\tau_1 = 0.0$ ps (0.61), $\tau_2 = 9.0$ ps (0.39). (d) 795 nm, $\tau = 8.5$ ps. (e) 801 nm, $\tau_1 = 18$ ps (0.58), $\tau_2 = 33$ ps (-0.42). (f) 754 nm, $\tau_1 = 9.1$ ps (0.77), $\tau_2 = 34$ ps (-0.23). The residuals from the fits are plotted above each panel. Conditions were as in Fig. 1. As discussed in the text, the values of τ_2 in (e) and (f) are too long to be constrained tightly by the measurements, and uncertainties in τ_2 propagate to τ_1.

before subtraction in order to correct for the increasing population of excited molecules with time. This normalization cannot be done unambiguously in the absence of independent information on the time-dependence of the excitation. However, if the spectra collected near 0 ps and 1.5 ps are normalized arbitrarily at 865 nm, the bleaching at the earlier time is slightly narrower and blue-shifted relative to the bleaching at 1.5 ps (Fig. 1b, inset).

Fig. 2b and f shows measurements of the kinetics in the 750-nm region. After an initial rise associated with formation of P*, the kinetics here are dominated by a component that bleaches with a time-constant of 9.5 ± 0.5 ps at 320 K, or 7.0 ± 0.3 ps at 296 K. This bleaching probably reflects reduction of BPh. Its kinetics are, within experimental error, indistinguishable from the decay kinetics of P*.

The kinetics in the region between 790 and 815 nm (Fig. 2c–e) are similar to the kinetics at 750 nm, but also include two additional components. Near 813 nm, there is an indication of a very fast bleaching and recovery during the excitation pulse (Fig. 2c). This probably is analogous to the 400-fs component that has been observed previously in RCs of *Rb. sphaeroides* and *Rp. viridis* under non-selective excitation [7,9,14,19,51]. Near 800 nm, there also is a much slower kinetic component, which appears as a gradual absorbance increase (Fig. 2e). A similar slow absorbance increase at long times is seen on the long-wavelength side of the 750-nm band (Fig. 2f). A comparison of the absorbance changes associated with the formation of $P^+H_L^-$ and $P^+Q_A^-$ [38,41] suggests that the slow components reflect the transfer of an electron from H_L^- to Q_A. The time constant for the absorbance increase is not determined reliably from the present data but, in most of the fits, is on the order of several hundred picoseconds, as expected for electron transfer to the quinone [41].

Time constants obtained from multiexponental fits of the data between 790 and 815 nm varied somewhat with wavelength, particularly at wavelengths close to 800 nm. At 801 nm, after the initial absorbance increase that accompanies the formation of P*, the ensuing absorbance decrease occurs with an apparent time constant of about 18 ps, which is about twice as long as the time constants measured at 921 or 754 nm (Fig. 2e). With increasing wavelength, the time constant for the absorbance decrease becomes smaller until it is essentially the same as that for the decay of P* as seen in the stimulated-emission band (Fig. 2c). Time constants for electron transfer between P* and H_L in *Rb. sphaeroides*, and between H_L^- and Q_A in both *Rb. sphaeroides* and *C. aurantiacus*, also have been reported to vary with wavelength in the 760 and 800 nm regions [15,21,41]. In the present case, this could be at least in part an artifact of the curve-fitting, resulting from incomplete resolution of the absorbance decrease and the subsequent slow absorbance increase associated with electron transfer to Q_A.

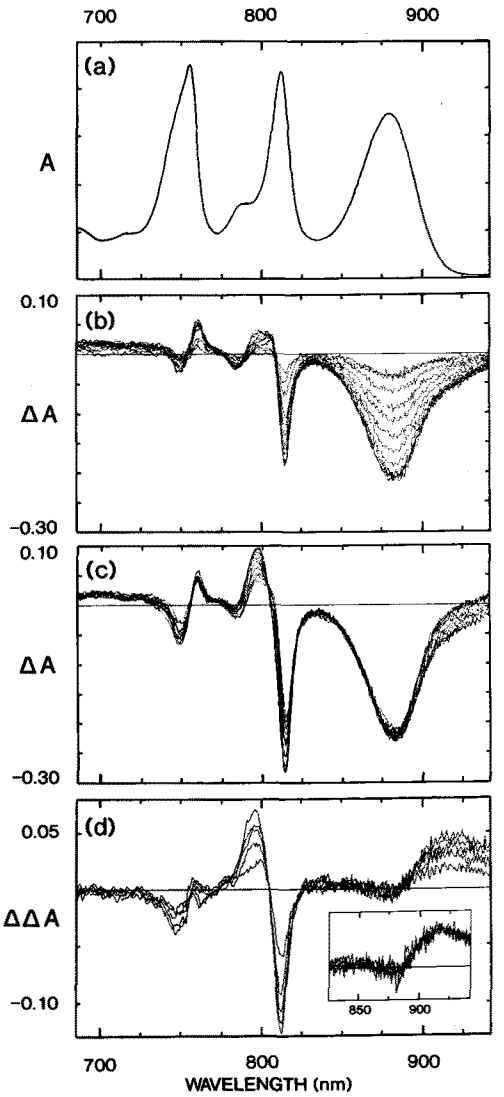

Fig. 3. Spectra of *C. aurantiacus* RCs in PVA films at 80 K. (a) Ground-state absorption spectrum. (b) Difference spectra at times between −1.0 ps and 1.5 ps. Sample *A* at 813 nm = 1.2 at 296 K. (c) Difference spectra at selected times between 1.5 and 90 ps. (d) Stimulated-emission spectra obtained by subtracting spectra measured at 1, 1.75, 3, 4.25, and 8.75 ps from an averaged spectrum between 70 and 90 ps. Inset: same spectra, normalized at 920 nm.

Spectra and kinetics at low temperatures

Fig. 3a shows the ground-state absorption spectrum of *C. aurantiacus* RCs in a PVA film at 80 K, and Fig. 3b and c shows difference spectra measured in a film at times between −1 and 90 ps after excitation. The difference spectra are qualitatively similar to those obtained at higher temperatures, but the bands sharpen and the 865-nm band shifts to longer wavelengths, yielding better spectral resolution. Spectra obtained during the first 1.5 ps (Fig. 3b) are characterized by

bleaching of the long-wavelength band at 880 nm, stimulated emission near 920 nm, and small absorbance decreases at 815, 785, and 750 nm. Absorbance increases occur to the blue of 740 nm, and at 760, 804, and 797 nm. Spectra collected at later times (Fig. 3c) show a decay of the stimulated emission, further absorbance decreases at 750 and 815 nm, and a further absorbance increase at 797 nm.

Fig. 4 shows the kinetics at selected wavelengths at 80 K. The decay of stimulated emission at 927 nm is shown in Fig. 4a, along with a single-exponential fit to the data. The decay is clearly non-exponential. As shown in Fig. 4b, a biexponential function gives a more satisfactory fit. For RCs in PVA films at 80 K, biexponential fits at various wavelengths across the stimulated-emission band from 910 to 935 nm give average time constants of 3.0 ± 0.1 ps and 32 ± 12 ps. The ratio of the amplitude of the fast component to that of the slow is 1.7 ± 0.2. The speed and relative contribution of the fast component both tend to increase slightly with wavelength across the spectrum. However, stimulated-emission spectra at various times between 1 and 9 ps after the excitation pulse (Fig. 3d) are indistinguishable within the experimental noise when normalized at 920 nm (Fig. 3d, inset).

The kinetics measured at low temperatures could also be fit satisfactorily by convolving the excitation function with a stretched-exponential function:

$$S(t) = E(t-\delta) \otimes (A\, e^{-(t/\tau_0)^{\alpha}} + B) \tag{2}$$

where A, τ_0, α and B are constants, and $0 < \alpha \leq 1$ [16]. Stretched-exponential and multiexponential fits to kinetic data are often indistinguishable [52], and this proved to be true in the present case; Fig. 4b shows only the residuals from a stretched-exponential fit for comparison with the residuals from the biexponential fit to the same data. Stretched-exponential fits in the stimulated-emission band at 80 K yielded average values of $\tau_0 = 4.1 \pm 1.2$ ps and $\alpha = 0.45 \pm 0.06$. If the stretched exponential is equated to a continuous distribution of exponential relaxation functions, the mean lifetime, τ_{AV}, is given by

$$\tau_{AV} = (\tau_0/\alpha)\Gamma(1/\alpha) \tag{3}$$

where Γ is the gamma function [53]. When $\alpha = 1$ the stretched exponential collapses to a single exponential and $\tau_{AV} = \tau_0$. Fits to the stimulated emission at 80 K gave $\tau_{AV} = 11 \pm 1$ ps, with no significant dependence on wavelength. Possible interpretations of the stretched-ex-

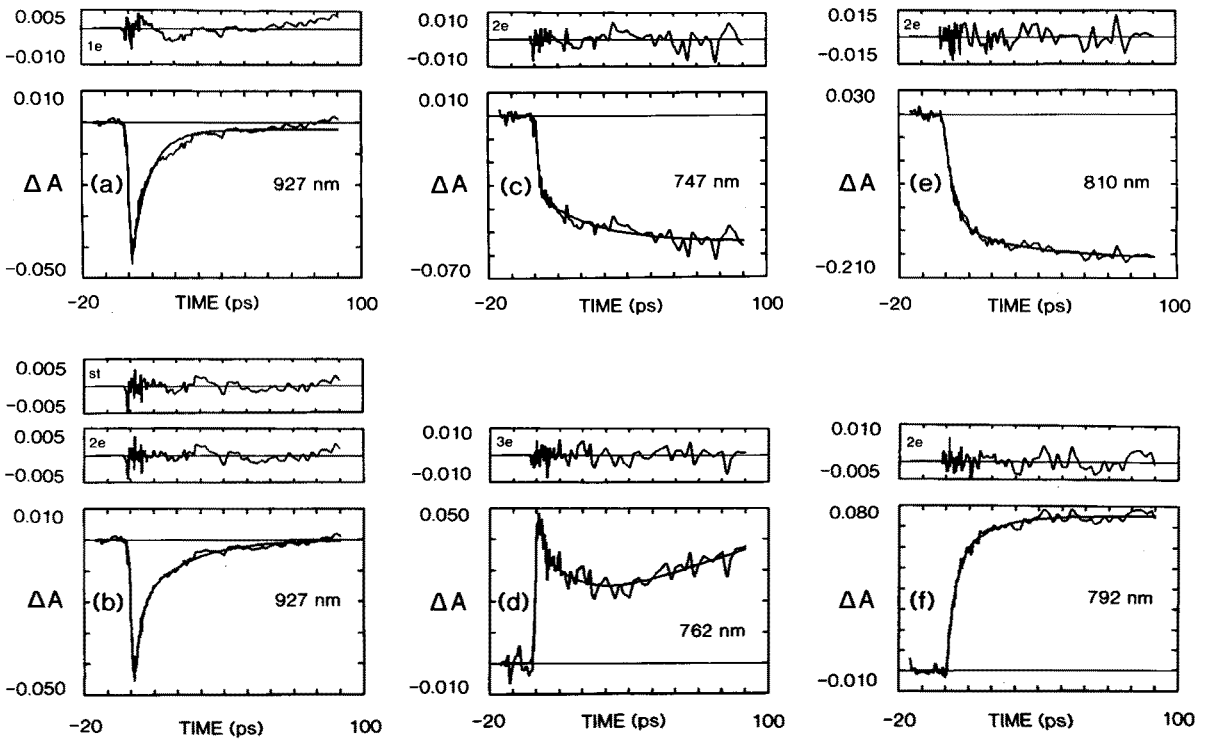

Fig. 4. Kinetics at 80 K. Conditions as in Fig. 3. The traces in (a) and (b) are averaged over 10 nm; those in (c), over 8 nm; and those in (d)–(f), over 4 nm. The smooth curves and the corresponding plots of residuals show multiexponential expressions with the following time constants (1e, = single exponential, 2e = biexponential, 3e = triexponential; numbers in parentheses are relative amplitudes): (a) 927 pm, $\tau = 8.0$ ps [the systematic departures of the residuals from zero indicate that this fit is unsatisfactory]. (b) 927 nm, $\tau_1 = 2.6$ ps (0.61), $\tau_2 = 20$ ps (0.39) [the upper panel of residuals, labeled ST, are for a stretched exponential with $\tau_0 = 2.7$ ps and $\alpha = 0.40$]. (c) 747 pm, $\tau_1 = 1.0$ ps (0.60), $\tau_2 = 24$ ps (0.40). (d) 762 nm, $\tau_0 = 1.7$ ps (0.17), $\tau_2 = 25$ ps (0.35), $\tau_3 = 83$ ps (-0.48). (e) 810 nm, $\tau_0 = 4.1$ ps (0.76), $\tau_2 = 33$ ps (0.24). (f) 792 nm, $\tau_1 = 2.9$ ps (0.68), $\tau_2 = 14$ ps (0.32). The data do not put tight constraints on the values of the parameters in (d).

ponential function will be considered in the Discussion.

Stretched-exponential fits to the high-temperature data discussed above yielded values of $\tau_0 = 9.1 \pm 0.4$ ps, $\alpha = 1.0 \pm 0.1$ and $\tau_{AV} = 9.1 \pm 0.3$ ps at 320 K, and $\tau_0 = 6.2 \pm 1.2$ ps, $\alpha = 0.82 \pm 0.14$ and $\tau_{AV} = 7.2 \pm 0.4$ ps at 296 K. The values of τ_{AV} are essentially identical to the time constants obtained from the single-expontial fits. At these temperatures, τ_{AV} increases by about 1 ps in going to longer wavelengths across the emission band, as expected from the single-exponential fits.

Because the absorbance changes in the 750- and 813-nm regions are expected to include several kinetic components, only multiexponential fits were used here. Fig. 4c shows the kinetics of the bleaching at 747 nm. With PVA films at 80 K, biexponential fits to the kinetics in this region yield average time constants of 1.7 ± 0.7 ps and 23 ± 3 ps. These values are shorter than the time constants measured in the stimulated-emission band, but probably are less reliable as measures of the initial electron-transfer kinetics. The faster component is likely to be perturbed by the instantaneous absorbance decrease that results from the excitation (Figs. 3b and 4c), and the slower one by absorbance changes associated with electron transfer from H_L^- to Q_A.

As in the experiments at higher temperatures, an additional kinetic component that probably reflects electron transfer to Q_A becomes prominent on the long-wavelength side of the 750-nm band and near 800 nm. At 762 nm (Fig. 4d), an instantaneous absorbance increase is followed by an absorbance decrease and then by an absorbance increase with a time constant on the order of 100 ps. Triexponential fits yield two components for the absorbance decrease, with time constants that are similar to those of the two components measured in the stimulated-emission band. Between 785 and 820 nm, the fits again yield two kinetic components that are qualitatively similar to those seen in the stimulated-emission band (Figs. 4e and f). The shorter time constant is essentially independent of wavelength, and has an average value of 2.8 ± 0.2 ps. The slower component varies with wavelength, probably in part because of distortion by electron transfer to Q_A.

The decay kinetics of P* also were measured with RCs in PVA films at intermediate temperatures. As mentioned above, data obtained with films at 297 K could be fit by either a single exponential or a biexponential function. With films at 189 and 137 K, as at 80 K, single-exponential fits were clearly unsatisfactory, and much better fits were obtained with either biexponential or stretched-exponential expressions. The time constants extracted from the biexponential fits were 4.0 ± 1.2 ps and 15 ± 6 ps at 189 K, and 3.5 ± 0.8 ps and 27 ± 15 ps at 137 K. The ratio of the amplitude of the fast component to that of the slow did not vary appreciably between 80 and 297 K, and had an average value of 1.6 ± 0.2. Fig. 5 shows plots of the rate constants (reciprocal time constants) of the two components as functions of temperature. The rate constant of the faster component increases as the temperature is lowered to 80 K, whereas that of the slower component decreases.

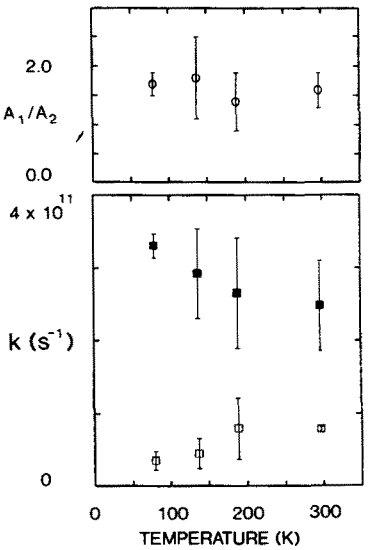

Fig. 5. Temperature dependence of the macroscopic rate constants ($k_i = 1/\tau_i$) and relative amplitudes (A_i) obtained by biexponential fits to the decay of the stimulated emission from RCs in PVA films. ■, k_1; □, k_2; ○ (upper panel), A_1/A_2.

Fig. 6 shows the temperature dependence of the parameters obtained by fitting the data to the stretched-exponential function. As the temperature is lowered, α decreases and k_0 ($1/\tau_0$) increases. The mean rate constant k_{AV} ($1/\tau_{AV}$) increases as the temperature is reduced from 320 K to 297 K, but then decreases.

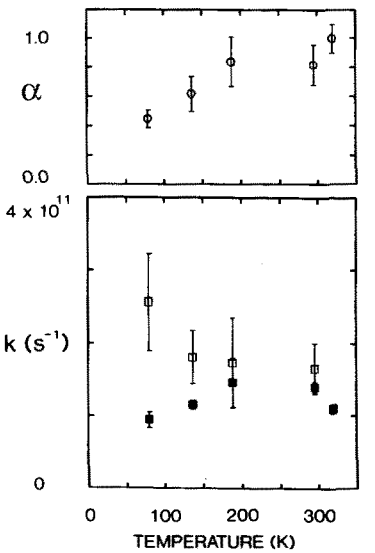

Fig. 6. Temperature dependence of stretched-exponential parameters for the decay of the stimulated emission. Values below 296 K are for PVA films; the value at 296 K is an average of film and solution data; and that at 320 K is for solution. □, k_0 ($1/\tau_0$); ■, k_{AV} ($1/\tau_{AV}$); ○ (upper panel), α.

To investigate one possible explanation for the non-exponential decay of P*, the effect of pH on the kinetics was examined. The charge-recombination reaction of $P^+Q_A^-$ in *Rp. viridis* exhibits biexponential kinetics that depend on the pH [54,55], and in *C. aurantiacus* it has been proposed that an ionized aspartic acid residue near P influences the rate of electron transfer from P* [56]. This suggests that frozen RCs might exist as a mixed population in several different protonation states and that the decay of P* varies among these states. To test this hypothesis, RC solutions in glycerol/buffer mixtures were prepared at pH 7.0, 7.8 and 9.4 (measured at 296 K) and were examined after cooling to 80 K. As in PVA films, the decay of the stimulated emission at 80 K was non-exponential. At each pH, biexponential fits to data from a single experiment yielded time constants of approx. 4 ps and 35 ps, with relative amplitudes of about 1.5 : 1 (data not shown). Thus, the decay of P* in RCs in 60% glycerol is similar to the decay in PVA films, and the kinetics are not altered appreciably by changing the pH over the range of 7.0 to 9.4 before the sample is cooled.

Discussion

*Absorbance changes associated with the formation of P**

The initial absorbance changes measured at high temperatures include absorbance decreases at 783 and 815 nm and increases at 762 and 802 nm, in addition to the bleaching of the long-wavelength (865 nm) band of P (Fig. 1b). The spectra obtained at low temperatures show similar features, along with an absorbance decrease at 750 nm (Fig. 3b). Most of these features are seen also in the difference spectra obtained by oxidizing P, or by converting it to a triplet state [29,36–43,57]. These absorbance changes probably reflect the loss of the absorption bands of P, disruption of exciton interactions of P with the other pigments, and the formation of new absorption bands of P*. Theoretical calculations based on the *Rp. viridis* crystal structure have suggested that some of the absorption bands of P and the other pigments can be strongly mixed [42,58–60]. However, these theoretical analyses vary in their treatments of short-range intermolecular interactions, and there is no concensus on the detailed description of the spectroscopic properties for any species of bacteria. The present measurements of spectral perturbations that result from exciting P should help to enlarge the data base for testing such calculations.

The bleaching near 790 and 813 nm in the spectra measured near 0 ps suggests that P makes significant contributions to the absorption bands at these wavelengths in the ground-state spectrum. Although the initial absorbance changes that we measured in the 813 nm region are complicated by the transient bleaching due to nonselective excitation of the RCs, Martin et al. [61] observed similar absorbance changes when they excited *C. aurantiacus* RCs directly in the long-wavelength absorption band of P. The 790 nm band cannot be described simply as the high-energy Q_y exciton band of P, because its transition dipole is nearly parallel to the transition dipole of the low-energy (865 nm) band, and both bands have positive rotational strengths [36–38]. Nor is the 790 nm band likely to be a simple vibrational shoulder of the 813 nm band, because these two transitions have opposite circular dichroism [36,38].

The absorbance rise at 762 nm at early times suggests that that the long-wavelength absorption band of P borrows intensity from the Q_y transition of the adjacent BPh on the M side. The cessation of this borrowing when P is excited would result in an absorbance increase in the 762 nm region. But observations of similar features in the P^+ and $P^+Q_A^-$ spectra of *Rb. sphaeroides* RCs [38,62] suggest that the absorbance changes in this region involve at least one of the BPhs that are distal to P. Vasmel et al. [42] have suggested that the absorbance changes in the $P^+Q_A^-$ spectrum of *C. aurantiacus* reflect a change in exciton interactions between the two BPhs on the M side.

Kirmaier and Holten [13,14] noted that the formation of P* in *Rb. capsulatus* causes little or no bleaching of the 800-nm absorption band of the ground-state spectrum. They concluded that the transitions of P are not strongly mixed with the Q_y transitions of the accessory BChls. The extent of this mixing could, of course, vary among different species of bacteria. However, interpretations of the absorbance changes associated with the excitation of P also could be complicated by contributions from the absorption bands of P*. When monomeric BChl is excited in vitro, the excited molecule has a very broad absorption band in the region of the Q_y transition [50].

*Possible origins of the non-exponential decay of P**

When *C. aurantiacus* RCs are excited at physiological temperatures, the decay of the stimulated emission from P* can be described well by a single-exponential function. The absorbance decrease at 750 nm, which is associated with reduction of BPh, occurs with similar kinetics. At temperatures of 189 K or below, the kinetics in both bands are clearly nonexponential. Since the two components obtained by biexponential fits converge as the temperature is raised (Fig. 5), it is possible that the decay at high temperatures also is nonexponential, but that the faster and slower components are more difficult to resolve.

There are several possible ways to account for the complex kinetics seen at low temperatures. First, as discussed by Nagarajan et al. [16], a time-dependent shifting of the stimulated-emission spectrum could complicate measurements of the true decay kinetics of P*,

leading to an artifactual appearance of wavelength-dependent, non-exponential kinetics. However, a small shift of the spectrum would have little effect on the measurements at wavelengths near the emission maximum. With *C. aurantiacus* RCs in solution at room temperature, the shifting of the stimulated-emission spectrum that appears to occur during the first 1.5 ps evidently has only a small effect on the analysis of the decay kinetics of P*, because the decay is described well by a single exponential. At 80 K, the shifting of the stimulated-emission band during the experimental window appears to be too small to account for the non-exponential kinetics.

Another possibility would be that measurements of the kinetics are complicated by slow transfer of energy from the accessory BChls to P. This is a potential problem in the present work, because the 605 nm excitation flashes probably excited the accessory BChls in addition to P. On the basis of recent time-resolved fluorescence measurements, Müller et al. [63] have suggested that energy transfer from the accessory BChls to P requires about 3 ps in *C. aurantiacus*. They observed that the fluorescence appeared to shift to longer wavelengths during the first few picoseconds after excitation of RCs at room temperature. However, it seems likely that this observation is related to the shifting of the stimulated-emission spectrum, which probably occurs after the transfer of the excitation to P. The decay kinetics of P* probably are not influenced greatly by the rate of the initial transfer of energy, because Martin et al. [61] observed similar nonexponential kinetics when they excited *C. aurantiacus* RCs selectively in the long-wavelength absorption band of P.

Other possible interpretations of the nonexponential kinetics include (1) the reversible formation of an intermediate state such as $P^+B_L^-$ (2) transient reduction of one or more of the BPhs on the M-side, (3) relaxations of the excited state, (4) static heterogeneity, and (5) a random walk among conformational states. We shall discuss the main features of these models below. Although the models are not mutually exclusive, and the data do not allow a decisive choice among the alternatives, the two models involving static heterogeneity or a random walk among conformational states appear to offer the most satisfactory explanations of the nonexponential kinetics. The latter has the additional advantage of accounting simply for the opposite effects of temperature on the faster and slower components of the kinetics.

(1) Intermediate formation of $P^+B_L^-$. Shuvalov et al. [43] have suggested that P* first transfers an electron to B_L, with a time constant of 10 ps in *C. aurantiacus* at room temperature, and that B_L^- reduces H_L in 3 ps. This scheme was based on the observation that, when RCs were excited with a flash lasting about 33 ps, a bleaching near 813 nm appeared to be prominent at early times during the flash. The time constant for the bleaching in the 813 nm band was reported to be 9 ps, whereas the time constants for the bleaching in the BPh band near 750 nm and the decay of stimulated emission were both 14 ps [43].

The decay time constant of 7.1 ps that we measured for the stimulated emission at 296 K is shorter than the value reported by Shuvalov et al., probably because of our use of shorter pulses. The results described by Shuvalov et al. may have been complicated by electron transfer from H_L^- to Q_A during their relatively broad pulses [10]. In addition, their analysis is subject to the uncertainties inherent in normalizing spectra to correct for changes in the extent of excitation (see above), and it could have been distorted by the instantaneous bleaching at 812 due to disruption of exciton interactions. In the present work, we did not detect any absorbance changes that could be attributed unambiguously to the transient formation of $P^+B_L^-$. There was an additional rapid bleaching and recovery in the region of 813 nm (Fig. 2c), but this probably resulted from our nonselective excitation of the RCs [7,14,18,19,51]. The dependence of the time constants on wavelength in the region of 800 nm could reflect the transient formation of an intermediate state, but also could result from an incomplete resolution of the slower absorbance changes associated with electron transfer from H_L^- to Q_A. However, our results do not rule out transient formation of $P^+B_L^-$, provided that the transfer of an electron from B_L^- to H_L is much faster than the transfer from P* to B_L.

To investigate whether the reversible formation of $P^+B_L^-$ could account for the non-exponential decay kinetics of P*, we considered the kinetic model shown in Fig. 7a. The kinetic equations for a three-state model of this type can be solved analytically [64,65], and exact solutions for the microscopic rate constants k_1, k_2 and k_3 can be obtained in terms of the time constants and relative amplitudes of the two components measured in the stimulated-emission region. Fig. 7a shows the calculated relative populations of the three states as functions of time after δ-function excitation at 297 and 80 K. At both temperatures, the model predicts that the formation of $P^+H_L^-$, as measured by the bleaching of the band at 750 nm, would be considerably slower than the decay of P*; this was not seen experimentally (Fig. 4c). Thus, the non-exponential decay of P* apparently cannot be explained simply by the reversible formation of $P^+B_L^-$.

(2) Reversible reactions on the M side. Complex decay kinetics of P* could result from the reduction of a BPh on the M side of the RC, in addition to H_L. Although our measurements in the 750 nm region give no indication of the transient reduction of a BPh other than H_L, the overlapping of the Q_y absorption bands of the different BPhs might make this difficult to detect.

Aumeier et al. [66] have reported that the decay kinetics of the flash-induced bleaching at 533 nm, where one might expect to detect the transient reduction of either of the BPhs on the M side, are essentially the same as the decay kinetics of $P^+H_L^-$ measured at 540 nm. At 85 K, the decay at both wavelengths occurred with a time constant of about 300 ps in RCs that contained Q_A, and slowed to longer than 5 ns if Q_A was removed [66]. Aumeier et al. concluded that the absorbance changes at 533 nm result indirectly from the formation and decay of $P^+H_L^-$, and do not reflect electron transfer to the M side. However, their observations do not exclude the latter interpretation, provided that this process is reversible. A model that includes a reversible reaction of this nature is shown in Fig. 7b. The model implies that electron transfer from P* to H_L slows down with decreasing temperature, while electron transfer to H_M speeds up.

The decay times expected for $P^+H_M^-$ in the model of Fig. 7b are much shorter than the time constant of 300 ps that Aumeier et al. [66] measured at 533 nm. Thus, there appears to be no indication that electron-transfer to the M side occurs with kinetics that would explain the nonexponential decay of P*.

(3) Relaxations in the excited state. The rate of electron transfer could change with time if P* undergoes relaxations that alter the electrostatic or electronic interactions of the pigments with each other or with their surroundings. Fig. 7c shows a model in which P* relaxes from its initial form ($P^*_{(1)}$) to a form that is less favorable for electron transfer ($P^*_{(2)}$). To solve for the three microscopic rate constants in this model, it is necessary to assume that the relaxation is irreversible, since the experimental observations provide only three parameters. However, the introduction of some reversibility would not greatly affect the results. The putative relaxation is calculated to decrease the rate constant for the formation of $P^+H_L^-$ by a factor of 2.4 at 297 K, and by a factor of 6.2 at 80 K. The model requires the relaxation to occur with a rate constant of about $6.5 \cdot 10^{10}$ s^{-1} at 297 K, and $11 \cdot 10^{10}$ s^{-1} at 80 K. Such an increase in the rate of relaxation with decreasing temperature seems unlikely, because nuclear relaxations generally slow down at low temperatures.

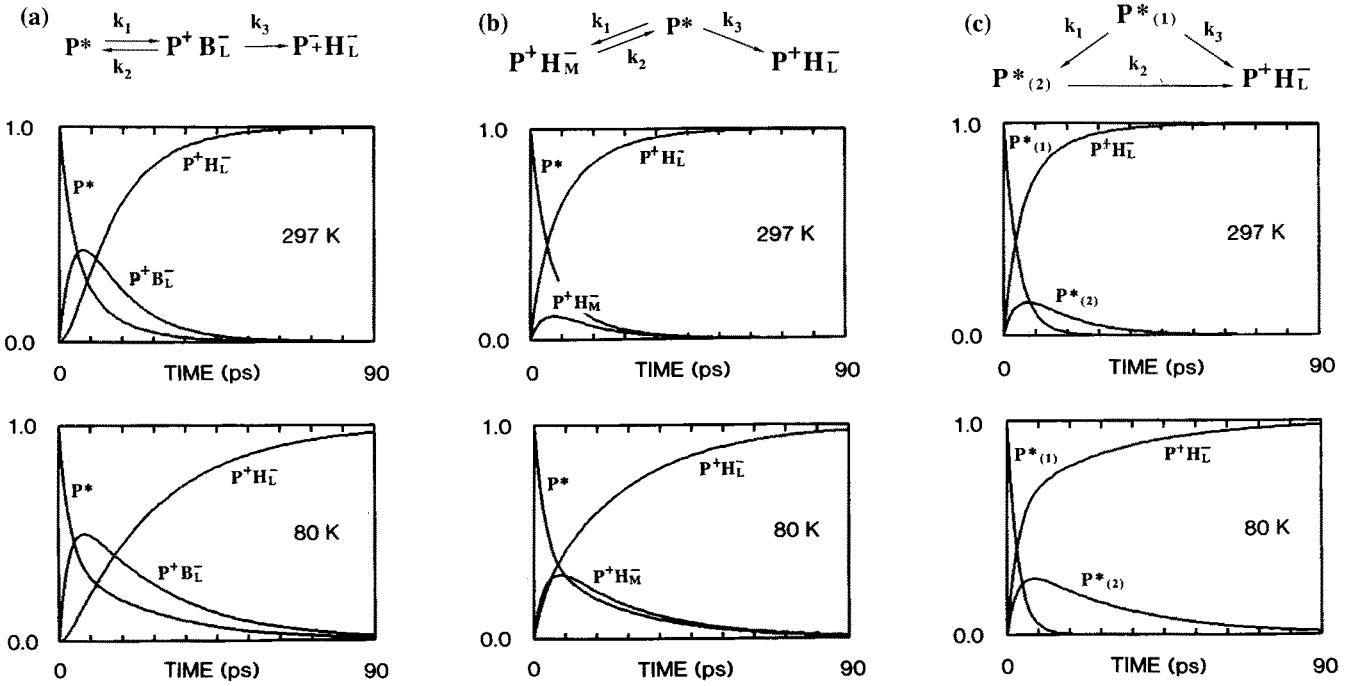

Fig. 7. (a) Relative populations of P*, $P^+B_L^-$, and $P^+H_L^-$ calculated for a sequential electron-transfer model at 297 K and 80 K. The model is at the top. The microscopic rate constants (k_1, k_2 and k_3) are obtained by solving the rate equations in terms of the observed biexponential decay rate constants for P* ($24.9 \cdot 10^{10}$ s^{-1} and $7.9 \cdot 10^{10}$ s^{-1} at 297 K; $33.1 \cdot 10^{10}$ s^{-1} and $3.5 \cdot 10^{10}$ s^{-1} at 80 K) and the ratio of the amplitudes of the fast and slow components (1.6 at both temperatures). The solutions for the rate constants are: $k_1 = 18.5 \cdot 10^{10}$ s^{-1}, $k_2 = 3.7 \cdot 10^{10}$ s^{-1} and $k_3 = 10.8 \cdot 10^{10}$ s^{-1} at 297 K, and $k_1 = 22.0 \cdot 10^{10}$ s^{-1}, $k_2 = 9.0 \cdot 10^{10}$ s^{-1} and $k_3 = 6.0 \cdot 10^{10}$ s^{-1} at 80 K. This analysis is based solely on the decay kinetics of P*, and does not incorporate any independent information on the formation or decay of $P^+B_L^-$. The figure is intended only to show that this model cannot, by itself, account for the decay kinetics of P*, because the predicted rise kinetics of $P^+H_L^-$ disagree with the measurements in the 750-nm region. (b) Relative populations of P*, $P^+B_L^-$, and $P^+H_L^-$ in a branched electron-transfer model. 'H_M' could designate either one or both of the two BPhs on the M side of the RC. The solutions for the microscopic rate constants are: $k_1 = 4.7 \cdot 10^{10}$ s^{-1}, $k_2 = 14.5 \cdot 10^{10}$ s^{-1} and $k_3 = 13.8 \cdot 10^{10}$ s^{-1} at 297 K, and $k_1 = 13.2 \cdot 10^{10}$ s^{-1}, $k_2 = 15.0 \cdot 10^{10}$ s^{-1} and $k_3 = 8.8 \cdot 10^{10}$ s^{-1} at 80 K. (c) Relative populations of P* and $P^+H_L^-$ in a model that includes unrelaxed and relaxed forms of P* ($P^*_{(1)}$ and $P^*_{(2)}$). In this model, the intensity of stimulated emission is proportional to $[P^*_{(1)}] + [P^*_{(2)}]$, or $1 - [P^+H_L^-]$. The solutions for the rate constants are: $k_1 = 6.5 \cdot 10^{10}$ s^{-1}, $k_2 = 7.9 \cdot 10^{10}$ s^{-1} and $k_3 = 18.4 \cdot 10^{10}$ s^{-1} at 297 K, and $k_1 = 11.4 \cdot 10^{10}$ s^{-1}, $k_2 = 3.5 \cdot 10^{10}$ s^{-1} and $k_3 = 21.7 \cdot 10^{10}$ s^{-1} at 80 K.

Relaxations of P* could explain the wavelength dependence of the kinetics in the stimulated-emission band, if the unrelaxed and relaxed species have different emission spectra. With PVA films at low temperatures, the emission decays most rapidly on the long-wavelength side of the band, which would imply that $P^*_{(2)}$ emits at shorter wavelengths than $P^*_{(1)}$. A shift in this direction is unexpected because the emission from BChl in vitro moves to longer wavelengths with time [50], and the emission from RCs in solution at higher temperatures appears to do likewise. However, a blue shift has been seen in RCs from a mutant strain of *Rb. sphaeroides* at low temperatures [16].

(4) Static heterogeneity. The biexponential description of the decay kinetics could be interpreted to mean that *C. aurantiacus* RCs exist in at least two discrete states. In this model, about 60% of the RCs exhibit a rate constant of approx. $25 \cdot 10^{10}$ s^{-1} for the decay of P* at 297 K, and 40% have a rate constant of $8 \cdot 10^{10}$ s^{-1}. The rate constant in the former population increases by about a factor of 1.3 as the temperature is lowered to 80 K, while the rate constant in the other population decreases by about a factor of 2.3 (Fig. 5). The exponential kinetics seen with RCs in solution could mean that RCs are more homogeneous under these condition, that there is less difference between the rate constants in their subpopulations, or that the subpopulations are able to interconvert more rapidly on the picosecond time scale.

A limitation of using multiexponential expressions to analyze kinetic processes is that the analysis indicates only the minimum number of components that are needed to fit the data. In the present case, we can say only that at least two terms are necessary to describe the decay of P*. In RCs of *Rb. sphaeroides*, the recombination kinetics of $P^+Q_A^-$ have been analyzed by using a power-law function to model a continuous distribution of kinetic components [67]. As noted above, the stretched-exponential function can be interpreted similarly by equating it to a distribution of exponential decays with time constants τ [53,68]:

$$e^{-(t/\tau_0)^\alpha} = \int_0^\infty f(\tau)\, e^{-t/\tau} d\tau \qquad \text{with} \int_0^\infty f(\tau)\, d\tau = 1 \tag{4}$$

For general α and τ_0, the shape of the normalized distribution function $f(\tau)$ is given by [68]

$$f(\tau) = \frac{-1}{\pi\tau} \sum_{j=0}^{\infty} \left\{ [-(\tau/\tau_0)^\alpha]^j \sin(j\pi\alpha) \frac{\Gamma(j\alpha+1)}{\Gamma(j+1)} \right\} \tag{5}$$

The mean time constant, τ_{AV}, defined as $\tau_{AV} = \int_0^\infty f(\tau)\tau\, d\tau$, can be obtained directly from τ_0 and α by Eqn. 3. Fig. 8 shows plots of the function $f(\tau)\tau/\tau_{AV}$ calculated by Eqns. 3 and 5 using the data on RCs in films at 189, 137 and 80 K. The distributions broaden as the temperature is lowered, suggesting that the decay of P* speeds up in some RCs and decreases in others.

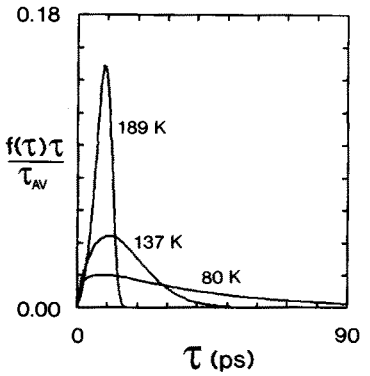

Fig. 8. The function $f(\tau)\tau/\tau_{AV}$ obtained by Eqns. 3 and 5, using the parameters τ_0 and α obtained from stretched-exponential fits of the stimulated emission from RCs at 189 K, 137 K and 80 K. Weighting $f(\tau)$ by τ gives a function that is well behaved as $\tau \to 0$. If the stretched-exponential function is interpreted in terms of a continuous distribution of time constants (Eqn. 4), $f(\tau)\tau/\tau_{AV}$ represents the relative contribution that a given value of τ makes to the mean decay time constant, τ_{AV}.

Several types of chemical heterogeneity could affect the decay of P*. Subpopulations could, for example, differ in the presence of phospholipids or colorless peptides, or in the amount of bound quinone. Heterogeneous protonation probably cannot account for the kinetics, because changing the pH over the range 7.0 to 9.4 had no significant effect on the relative amplitudes of the two decay components obtained from the biexponential fits.

Another possibility is that the subpopulations differ only in conformation. Conformational heterogeneity could lead to a distribution of electronic coupling strengths or electrostatic energies. Recent studies of mutant *Rb. sphaeroides* RCs have shown that replacing tyrosine M210 by phenylalanine or isoleucine results in non-exponential kinetics at low temperatures, suggesting that the tyrosine contributes to stabilizing the structure of the RC [16]. The homologous residue in *C. aurantiacus* is a leucine [26,28,69].

Static heterogeneity also could account for the wavelength dependence of the kinetics. At 80 K the increase in the decay rate constant on the long-wavelength side of the stimulated-emission band suggests that subpopulations with faster decay kinetics tend to emit at longer wavelengths. Previous workers have offered similar proposals to explain the wavelength dependence of kinetic measurements in the 800 nm region in *Rb. sphaeroides*, *Rp. viridis*, and *Rhodospirillum rubrum* [15,55,70]. Spectroscopic heterogeneity also has been described in absorption-detected-magnetic-resonance studies on several bacterial species, including *C. aurantiacus* [57,71]. Photochemical hole-burning studies on *Rb. sphaeroides* and *Rp. viridis* at low temperatures have shown that

inhomogeneous broadening of the long-wavelength band is greater in PVA films than in glycerol/water glasses [72]. We observed similar kinetics in the two media, but did not study glycerol/water mixtures in detail.

(5) Rapid interconversion among conformational states. Although the stretched-exponential function can be used to model a continuous distribution of exponentials as described above, the same function also arises naturally in systems that undergo random walks among a variety of states, with long-tailed distributions of pausing times between steps [73]. Models based on such random walks have been applied to a wide variety of physical phenomena, including dielectric relaxation in polymer glasses and electron transfer in frozen solutions [53,74], and transitions among hierarchical families of conformational states in proteins [75,76]. Thus, the stretched-exponential description of the kinetics of electron transfer might be interpreted as reflecting conformational interconversions that occur prior to electron transfer. The essence of this model is that the conformation of the RC fluctuates on the time scale of the electron-transfer reaction, and that electron transfer proceeds most rapidly from a particular conformation that is reached by a random walk. The slowing of conformational transitions with decreasing temperature would explain why the kinetics of electron transfer in the RC become most markedly nonexponential at low temperatures. We return to this point below.

The rate and temperature-dependence of electron transfer

At room temperature, the time constant for the decay of P* in *C. aurantiacus* RCs, 7 ps, is approximately twice as large as the time constants that have been measured in *Rb. sphaeroides*, *Rb. capsulatus* and *Rp. viridis*. Although fluorescence measurements have given a decay time constant of 7 ps for P* in *Rs. rubrum* [77], recent picosecond absorbance measurements give a time constant of approx. 3.5 ps in this species also (Nagarajan, V., unpublished observations).

In addition to the substitution of BPh for one of the BChls, RCs of *C. aurantiacus* differ from those of the other species at several amino acid residues that are probably close enough to the pigments so that they might influence the rate of electron transfer. Klevanik et al. [56] have suggested that electron transfer in *C. aurantiacus* is slowed by electrostatic effects of aspartic acid L281. The homologous residue in *Rb. sphaeroides* and *Rb. capsulatus* is a serine, and that in *Rp. viridis* is a glycine. But without more detailed structural information, it is not possible to predict whether or not the aspartic acid would be ionized at physiological pH. If the aspartate does influence the electron-transfer rate, then the insensitivity of the kinetics to pH indicates that the carboxyl group does not titrate in the pH range from 7.0 to 9.4. Another potentially important difference between the species is the replacement of glutamic acid L104 of *Rb. sphaeroides*, *Rb. capsulatus* and *Rp. viridis* by glutamine in *C. aurantiacus* [27]. The glutamic acid probably forms a hydrogen bond with H_L in the three former species, and replacing it by glutamine in mutant RCs of *Rb. capsulatus* decreases the rate of electron transfer at room temperature by about 30% [25]. Finally, a tyrosine residue (M210 in *Rb. sphaeroides*, M208 in *Rb. capsulatus* and *Rp. viridis*) is replaced by leucine M199 in *C. aurantiacus* [28]. When this residue was mutated to phenylalanine, leucine or isoleucine in *Rb. sphaeroides*, electron transfer was slowed by factors of between 3 and 7 at room temperature, and by larger factors at low temperatures [16,78]. Electrostatic calculations on the *Rp. viridis* crystal structure have suggested that the tyrosine may be important for lowering the energy of $P^+B_L^-$ [79].

In *Rb. sphaeroides* and *Rp. viridis*, the rate of the initial electron transfer increases with decreasing temperature [7,15,16,19,23]. This has been interpreted to mean that the potential energy surface of the radical-pair product state intersects the potential energy surface of P* near the latter's minimum [80,81], that thermal contraction at low temperatures decreases the distance between the reactants [17,60,82], or that RCs are heterogeneous at high temperatures but freeze into a conformation that is favorable for electron transfer at low temperatures [15].

The temperature dependence of the electron-transfer rate is more difficult to characterize in *C. aurantiacus* because the decay of P* is nonexponential at low temperatures. Fitting the decay to a biexponential expression gives one component that speeds up with decreasing temperature, in qualitative agreement with the kinetics in the other bacterial species, and a slower component that changes in the opposite direction (Fig. 5). Between 320 and 296 K, where the decay fits a single exponential, the rate constant increases with decreasing temperature. If the data are fit to a stretched-exponential function, and this is equated to a continuous distribution of exponentials, the distribution broadens with decreasing temperature (Fig. 8). The mean rate constant, k_{AV} increases as the temperature is reduced from 320 to 296 K, but decreases at temperatures below 189 K; k_0 increases monotonically (Fig. 6).

A variety of interpretations of the temperature dependence could be given, depending on which model is adopted to account for the nonexponential kinetics. In the model that invokes reduction of a BPh on the M side (Fig. 7b), the equilibrium constants calculated from the microscopic rate constants can be related to the free energy difference between P* and $P^+H_M^-$. The model implies that $P^+H_M^-$ lies about 0.3 kcal/mol above P* at 297 K, but that the two states are nearly isoenergetic at 80 K. Since the calculated value of k_3 decreases as the temperature is lowered, this model also implies that the electron-transfer step from P* to H_L is thermally

activated, which would contrast with the behavior seen in wild-type strains of *Rb. sphaeroides* and *Rp. viridis*. If the nonexponential kinetics reflect static heterogeneity, electron transfer would appear to slow down with decreasing temperature in one population of RCs, but to speed up in another population. This could reflect a difference in the energies of the $P^+B_L^-$ or $P^+H_L^-$ radical-pairs in the different populations.

The model that postulates a random walk among conformational states provides a particularly simple rationalization of the opposite effects of temperature on the faster and slower components of the decay. In this model, the faster components represent RCs that are already in the reactive conformation at the time of the excitation flash, or that reach this state after only a few steps. Electron transfer in these RCs could speed up with decreasing temperature just as it does in the purple bacteria. The slower components of the decay would represent RCs that take more extended walks before they reach the reactive conformation. In these RCs, lowering the temperature would slow down electron transfer by reducing the rate of conformational transitions. At extremely low temperatures, when the barriers to conformational transitions become insurmountable, the quantum yield of charge separation should decline. Whether or not such a decline occurs remains to be determined.

Acknowledgements

This work was supported by NSF grant PCM-86166563 to W.W.P. and USDA CRGO grant 88-272623480 to R.E.B. This is publication No. 62 from the Arizona State Univ. Center for the Study of Early Events in Photosynthesis. The Center is funded by U.S. DOE grant No. DE-FG02-88ER13969 as part of the USDA/DOE/NSF Plant Science Centers Program. We thank M. Larvie for technical help, N.W. Woodbury and D. Holten for helpful discussions, and J. Breton and A. Holzwarth for informing us of their recent unpublished work.

References

1 Woese, C.R. (1987) Microbiol. Rev. 51, 221–271.
2 Williams, J.C., Steiner, L.A. and Feher, G. (1986) Proteins: Struc. Func. Genet. 1, 312–325.
3 Deisenhofer, J., Epp, O., Miki, K., Huber, R. and Michel, H. (1985) Nature (London) 318, 618–624.
4 Chang, C.-H., Tiede, D., Tang, J., Smith, U., Norris, J. and Schiffer, M. (1986) FEBS Lett. 205, 82–86.
5 Allen, J.P., Feher, G., Yeates, T.O., Komiya, H. and Rees, D.C. (1987) Proc. Natl. Acad. Sci. USA 84, 5730–5734.
6 Allen, J.P., Feher, G., Yeates, T.O., Komiya, H. and Rees, D.C. (1987) Proc. Natl. Acad. Sci. USA 84, 6162–6166.
7 Woodbury, N.W., Becker, M., Middendorf, D. and Parson, W.W. (1985) Biochemistry 24, 7516–7521.
8 Martin, J.-L., Breton, J., Hoff, A.J., Migus, A. and Antonetti, A. (1986) Proc. Natl. Acad. Sci. USA 83, 957–961.
9 Breton, J., Martin, J.-L., Migus, A., Antonetti, A. and Orszag, A. (1986) Proc. Natl. Acad. Sci. USA 83, 5121–5125.
10 Kirmaier, C., Holten, D. and Parson, W.W. (1985) FEBS Lett. 185, 76–82.
11 Holzapfel, W., Finkele, U., Kaiser, W., Oesterhelt, D., Scheer, H., Stilz, H.U. and Zinth, W. (1989) Chem. Phys. Lett. 160, 1–7.
12 Holzapfel, W., Finkele, U., Kaiser, W., Oesterhelt, D., Scheer, H., Stilz, H.U. and Zinth, W. (1990) Proc. Natl. Acad. Sci. USA, 87, 5168–5172.
13 Kirmaier, C. and Holten, D. (1988) FEBS Lett. 239, 211–218.
14 Kirmaier, C. and Holten, D. (1988) Isr. J. Chem. 28, 79–85.
15 Kirmaier, C. and Holten, D. (1990) Proc. Natl. Acad. Sci. USA 87, 3552–3556.
16 Nagarajan, V., Parson, W.W., Gaul, D. and Schenck, C.C. (1990) Proc. Natl. Acad. Sci. USA 87, 7888–7892.
17 Kirmaier, C. and Holten, D. (1988) in The Photosynthetic Bacterial Reaction Center, Structure and Dynamics (Breton, J. and Verméglio, A., eds.), pp. 219–228, Plenum, New York.
18 Breton, J., Martin, J.-L., Petrich, J., Migus, A. and Antonetti, A. (1986) FEBS Lett. 209, 37–43.
19 Breton, J., Martin, J.-L., Fleming, G.R. and Lambry, J.-C. (1988) Biochemistry 27, 8276–8284.
20 Shuvalov, V.A. and Duysens, L.N.M. (1986) Proc. Natl. Acad. Sci. USA 83, 1690–1694.
21 Kirmaier, C., Holten, D. and Parson, W.W. (1985) Biochim. Biophys. Acta 810, 33–48.
22 Wraight, C.A. and Clayton, R.K. (1974) Biochim. Biophys. Acta 333, 246–260.
23 Fleming, G.R., Martin, J.-L. and Breton, J. (1988) Nature 333, 190–192.
24 Kirmaier, C., Holten, D. and Parson, W.W. (1985) Biochim. Biophys. Acta 810, 49–61.
25 Bylina, E.J., Kirmaier, C., McDowell, L., Holten, D. and Youvan, D.C. (1988) Nature 336, 182–184.
26 Ovchinnikov, Yu.A., Abdulaev, N.G., Zolotarev, A.S., Shmukler, B.E., Zargarov, A.A., Kutuzov, M.A., Telezhinskaya, I.N. and Levina, N.B. (1988) FEBS Lett. 231, 237–242.
27 Ovchinnikov, Yu.A., Abdulaev, N.G., Shmukler, B.E., Zargarov, A.A., Kutuzov, M.A., Telezhinskaya, I.N., Levina, N.B. and Zolotarev, A.S. (1988) FEBS Lett. 232, 364–368.
28 Shiozawa, J.A., Lottspeich, F., Oesterhelt, D. and Feick, R. (1989) Eur. J. Biochem. 180, 75–84.
29 Pierson, B.K. and Thornber, J.P. (1983) Proc. Natl. Acad. Sci. USA 80, 80–84.
30 Blankenship, R.E., Feick, R., Bruce, B.D., Kirmaier, C., Holten, D. and Fuller, R.C. (1983) J. Cell. Biochem. 22, 251–261.
31 Hale, M.B., Blankenship, R.E. and Fuller, R.C. (1983) Biochim. Biophys. Acta 723, 376–382.
32 Vasmel, H. and Amesz, J. (1983) Biochim. Biophys. Acta 724, 118–122.
33 Mancino, L.J., Hansen, P.L., Stark, R.E. and Blankenship, R.E. (1985) Biophys. J. 47, 2a.
34 Pierson, B.K., Thornber, J.P. and Seftor, R.E.B. (1983) Biochim. Biophys. Acta 723, 322–326.
35 Bruce, B.D., Fuller, R.C. and Blankenship, R.E. (1982) Proc. Natl. Acad. Sci. USA 79, 6532–6536.
36 Vasmel, H., Meiburg, R.F., Kramer, H.J.M., De Vos, L.J. and Amesz, J. (1983) Biochim. Biophys. Acta 724, 333–339.
37 Parot, P., Delmas, N., Garcia, D. and Verméglio, A. (1985) Biochim. Biophys. Acta 809, 137–140.
38 Shuvalov, V.A., Shkuropatov, A.Ya., Kulakova, S.M., Ismailov, M.A, and Shkuropatova, V.A. (1986) Biochim. Biophys. Acta 849, 337–346.
39 Kirmaier, C., Holten, D., Feick, R. and Blankenship, R.E. (1983) FEBS Lett. 158, 73–78.
40 Kirmaier, C., Holten, D., Mancino, L.J. and Blankenship, R.E. (1984) Biochim. Biophys. Acta 765, 138–146.

41 Kirmaier, C., Blankenship, R.E. and Holten, D. (1986) Biochim. Biophys. Acta 850, 275–285.
42 Vasmel, H., Amesz, J. and Hoff, A.J. (1986) Biochim. Biophys. Acta 852, 159–168.
43 Shuvalov, V.A., Vasmel, H., Amesz, J. and Duysens, L.N.M. (1986) Biochim. Biophys. Acta 851, 361–368.
44 Becker, M., Middendorf, D., Woodbury, N.W., Parson, W.W. and Blankenship, R.E. (1986) in Ultrafast Phenomena V (Fleming, G.R. and Siegman, A.E., eds.), pp. 374–378, Springer, Berlin.
45 Becker, M., Middendorf, D., Nagarajan, V., Parson, W.W., Martin, J.E. and Blankenship, R.E. (1990) in Current Research in Photosynthesis. Vol. 1 (Baltscheffsky, M., ed.), pp. 121–124, Kluwer, Dordrecht.
46 Pierson, B.K. and Castenholz, R.W. (1981) in The Prokaryotes: A Handbook of Habitats, Isolation, and Identification of Bacteria. Vol. 1 (Star, M.P., Stolz, H., Truper, H.G., Balows, A. and Schlegel, H.G., eds.), pp. 290–298, Springer, Berlin.
47 Blankenship, R.E., Trost, J.T. and Mancino, L.J. (1988) in The Photosynthetic Bacterial Reaction Center, Structure and Dynamics (Breton, J. and Verméglio, A., eds.), pp. 119–127, Plenum, New York.
48 Schenck, C.C., Parson, W.W., Holten, D., Windsor, M.W. and Sarai, A. (1981) Biophys. J. 36, 479–489.
49 Woodbury, N.W. (1986) Ph.D. Thesis, University of Washington.
50 Becker, M., Nagarajan, V., Middendorf, D., Shield, M.A. and Parson, W.W. (1990) in Current Research in Photosynthesis, Vol 1 (Baltscheffsky, M., ed.), pp 101–104, Kluwer, Dordrecht.
51 Petrich, J.W., Breton, J. and Martin, J.-L. (1987) in Primary Processes in Photobiology, Springer Proc. in Phys., Vol. 20 (Kobayashi, T., ed.), pp. 52–60, Springer, Berlin.
52 Marshall, D.B. (1989) Anal. Chem. 61, 660–665.
53 Plonka, A. (1988) Time Dependent Reactivity of Species in Condensed Media, Lect. Notes Chem., Vol. 40, Springer, Berlin.
54 Sebban, P. and Wraight, C.A. (1989) Biochim. Biophys. Acta 974, 54–65.
55 Baciou, L., Rivas, E. and Sebban, P. (1990) Biochemistry 29, 2966–2975.
56 Klevanik, A.V., Ganago, A.O., Shkuropatov, A.Y. and Shuvalov, V.A. (1988) FEBS Lett. 237, 61–64.
57 den Blanken, H.J., Vasmel, H., Jongenelis, A.P.J.M., Hoff, A.J. and Amesz, J. (1983) FEBS Lett. 161, 185–189.
58 Parson, W.W., and Warshel, A. (1987) J. Am. Chem. Soc. 109, 6152–6163.
59 Scherrer, P.O.J., and Fischer, S.F. (1988) in The Photosynthetic Bacterial Reaction Center, Structure and Dynamics (Breton, J. and Verméglio, A., eds.), pp. 319–329, Plenum, New York.
60 Friesner, R.A. and Won, Y. (1989) Biochim. Biophys. Acta 977, 99–122.
61 Martin, J.-L., Lambry, J.C., Ashokkumar, M., Michel-Beyerle, M.E., Feick, R. and Breton, J. (1991) in Ultrafast Phenomena VII (Harris, C.B. and Ippen, E.P., eds.), Springer, Berlin, in press.
62 Breton, J. (1988) in The Photosynthetic Bacterial Reaction Center, Structure and Dynamics (Breton, J. and Verméglio, A., eds.), pp. 59–69, Plenum, New York.
63 Müller, M.G., Griebenow, K. and Holzwarth, A.R. (1991) in Structure and Function of Bacterial Reaction Centers (Michel-Beyerle, M.E., ed.), Springer, Berlin, in press.
64 Frost, A.A. and Pearson, R.G. (1953) Kinetics and Mechanism pp. 160–164, John Wiley, New York.
65 Schenck, C.C., Blankenship, R.E. and Parson, W.W. (1982) Biochim. Biophys. Acta 680, 44–59.
66 Aumaier, W., Eberl, U., Ogrodnik, A., Volk, M., Scheidel, G., Feick, R. and Michel-Beyerle, M.E. (1990) in Current Research in Photosynthesis. Vol 1 (Baltscheffsky, M., ed.), pp. 133–136, Kluwer, Dordrecht.
67 Kleinfeld, D., Okamura, M.Y. and Feher, G. (1984) Biochemistry 23, 5780–5786.
68 Montroll, E.W. and Bendler, J.T. (1984) J. Stat. Phys. 34, 129–162.
69 Komiya, H., Yeates, T.O., Rees, D.C., Allen, J.P. and Feher, G. (1988) Proc. Natl. Acad. Sci. USA 85, 9012–9016.
70 Parot, P., Thiery, J. and Verméglio, A. (1987) Biochim. Biophys. Acta 893, 534–543.
71 Hoff, A. (1988) in The Photosynthetic Bacterial Reaction Center, Structure and Dynamics (Breton, J. and Verméglio, A., eds.), pp. 89–97, Plenum, New York.
72 Johnson, S.G., Tang, D., Jankowiak, R., Hayes, J.M., Small, G.J. and Tiede, D.M. (1990) J. Phys. Chem. 94, 5849–5855.
73 Montroll, E.W. and West, B.J. (1979) in Fluctuation Phenomena (Montrol, E.W. and Lebowitz, J.L., eds.), pp. 61–175, North-Holland, Amsterdam.
74 Shlesinger, M.F. (1988) Annu. Rev. Phys. Chem. 39, 269–290.
75 Bendler, J.T. and Shlesinger, M.F. (1985) Macromolecules 18, 591–592.
76 Ansari, A., Berendzen, J., Bowne, S.F., Frauenfelder, H., Iben, I.E.T., Sauke, T.B., Shyamsunder, E. and Young, R.D. (1985) Nature 82, 5000–5004.
77 Freiberg, A.M., Godik, V.I., Kharchenko, S.G., Timpmann, K.E., Borisov, A.Yu. and Rebane, K.K. (1985) FEBS Lett. 189, 341–344.
78 Finkele, U., Lauterwasser, C., Zinth, W., Gray, K.A. and Oesterhelt, D. (1990) Biochemistry 29, 8517–8521.
79 Parson, W.W., Chu, Z.-T. and Warshel, A. (1990) Biochim. Biophys. Acta 1017, 251–272.
80 Bixon, M. and Jortner, J. (1989) Chem. Phys. Lett. 146, 17–20.
81 Warshel, A., Chu, Z.-T. and Parson, W.W. (1990) Science 246, 112–116.
82 Scherrer, P.O.J., Fischer, S.F., Hörber, J.K.H. and Michel-Beyerle, M.E. (1985) in Antennas and Reaction Centers of Photosynthetic Bacteria (Michel-Beyerle, M.E., ed.), pp. 131–137, Springer, Berlin.